

Supporting Information

Incorporating Semiflexible Linkers into Double-Cable Conjugated Polymers via Click Reaction

Zhaofan Yang,^a Shijie Liang,^a Baiqiao Liu,^a Jing Wang,^c Fan Yang,^{*b} Qiaomei Chen,^{*a} Chengyi Xiao,^a Zheng Tang,^c and Weiwei Li^{*a}

- ^a Beijing Advanced Innovation Center for Soft Matter Science and Engineering & State Key Laboratory of Organic-Inorganic Composites, Beijing University of Chemical Technology, Beijing 100029, China. E-mail: chenqm@mail.buct.edu.cn or liweiwei@iccas.ac.cn
- ^b College of Chemistry, Chemical Engineering and Materials Science, Collaborative Innovation Center of Functionalized Probes for Chemical Imaging in Universities of Shandong, Key Laboratory of Molecular and Nano Probes, Ministry of Education, Shandong Normal University, Jinan 250014, P. R. China. E-mail: yangfan1180@sdu.edu.cn
- ^c Center for Advanced Low-dimension Materials, College of Materials Science and Engineering, Donghua University, Shanghai 201620, P. R. China.

Contents

1. Materials and measurements
2. GPC curve
3. TGA curve
4. Absorption spectra
5. CV curve
6. Solubility test
7. Solar cells performance
8. NMR and MS of the compounds

1. Materials and measurements

All reagents and solvents were purchased from commercial sources and used without further purification. $^1\text{H-NMR}$ and $^{13}\text{C-NMR}$ spectra were recorded at 400 MHz on a Bruker AVANCE spectrometer with tetramethylsilane (TMS) as the internal standard. High resolution mass spectra (HRMS) were measured on a Bruker ultrafleXtreme MALDI TOF. The Molecular weight was determined with GPC at 150 °C on a PL-GPC 220 system using a PL-GEL 10 μm MIXED-B LS 300* column and 1,2,4-trichlorobenzene (TCB) as the eluent against polystyrene standards. TGA measurement was performed on a Perkin-Elmer Pyris6. DSC measurement was performed on a Perkin-Elmer DSC8000. Optical absorption spectra were recorded on a HITACHI U-2910 spectrometer with a slit width of 2.0 nm and a scan speed of 1000 nm min $^{-1}$. Cyclic voltammetry was performed under an inert atmosphere at a scan rate of 0.1 V s $^{-1}$ and 1 M tetrabutylammonium hexafluorophosphate in acetonitrile as the electrolyte, a glassy-carbon working electrode coated with samples, a platinum-wire auxiliary electrode, and an Ag/AgCl as a reference electrode.

GIWAXS measurements were performed at beamline 7.3.3 at the Advanced Light Source. Samples were prepared on Si substrates using identical blend solutions as those used in devices. The 10 keV X-ray beam was incident at a grazing angle of 0.12 -0.16, selected to maximize the scattering intensity from the samples. The scattered x-rays were detected using a Dectris Pilatus 2M photon counting detector. Atomic force microscopy (AFM) images were recorded using a Bruker-Fastscan in tapping mode under ambient conditions.

Photovoltaic devices with inverted configuration were made by spin-coating a ZnO sol-gel at 4000 rpm for 30 s onto pre-cleaned, patterned ITO substrates. The photoactive layer was deposited by spin coating CB solution containing the polymer and the appropriate amount of DIO as processing additive in the N $_2$ -filled glove box. MoO $_3$ (4 nm) and Ag (80 nm) were deposited by vacuum evaporation at ca. 4×10^{-5} Pa as the back electrode.

The active area of the cells was 0.04 cm 2 . The J - V characteristics were measured by a Keithley 2400 source meter unit under AM1.5G spectrum from a solar simulator (Enlitech model SS-F5-3A). Solar simulator illumination intensity was determined at 100 mW cm $^{-2}$ using a monocrystal silicon reference cell with KG5 filter. Short circuit currents under AM1.5G conditions were estimated from the spectral response and convolution with the solar spectrum. The external quantum efficiency was measured by a Solar Cell Spectral Response Measurement

System QE-R3011 (Enli Technology Co. Ltd.). The thickness of the active layers in the photovoltaic devices was measured on a Veeco Dektak XT profilometer.

Electroluminescence (EL) spectra was taken using a Kymera-328I spectrograph and an EMCCD purchased from Andor Technology (DU970P). Injection current used for EL was 1 mA/cm², and excitation wavelength used for the PL measurements was 500 nm. EQEEL measurements were done using a home-built setup using a Keithley 2400 to inject current to the solar cells. Emission photon-flux from the solar cells was recorded using a Si detector (Hamamatsu s1337-1010BQ) and a Keithley 6482 picometer.

Sensitive EQE measurements were done using a halogen lamp light source, chopped at a frequency of 173 Hz, a monochromator (Newport CS260), a Stanford SR830 lock-in amplifier, a Stanford SR570 current amplifier, and a set of long pass filters. Lamp intensity was calibrated using a Si detector (Hamamatsu s1337-1010BQ).

2. GPC curve

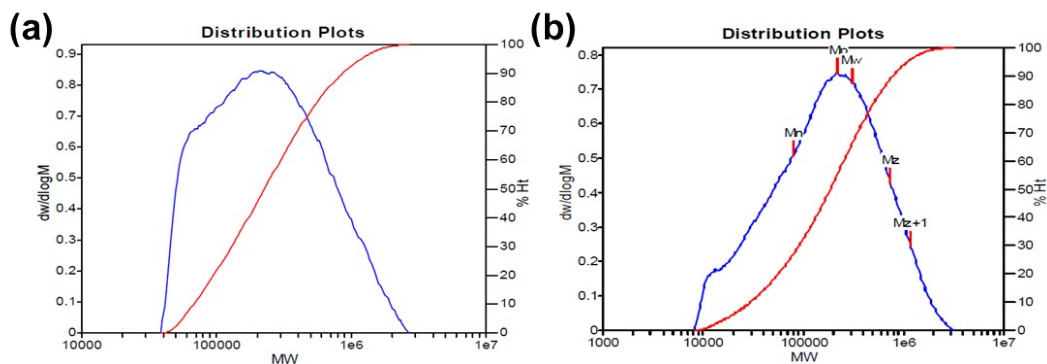


Figure S1. (a) GPC curve of **P1** recorded at 150 °C with TCB as eluent. (b) GPC curve of **P2** recorded at 150 °C with TCB as eluent.

3. TGA curve

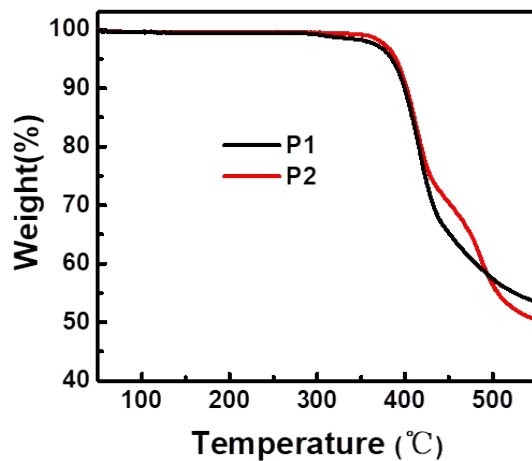


Figure S2. TGA plot with a heating rate of 10 °C/min under N₂ atmosphere.

4. Absorption spectra

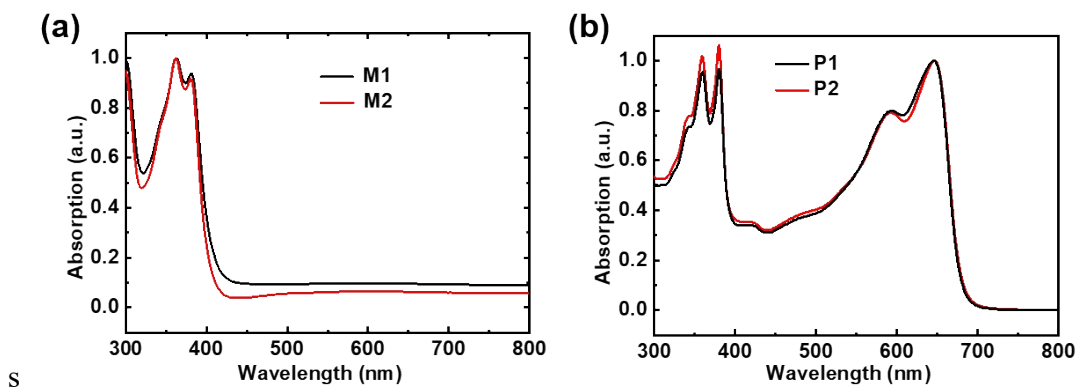


Figure S3. (a) Optical absorption spectra of the monomers M1 and M2. (b) Solution absorption spectra of polymers P1 and P2.

5. CV curves

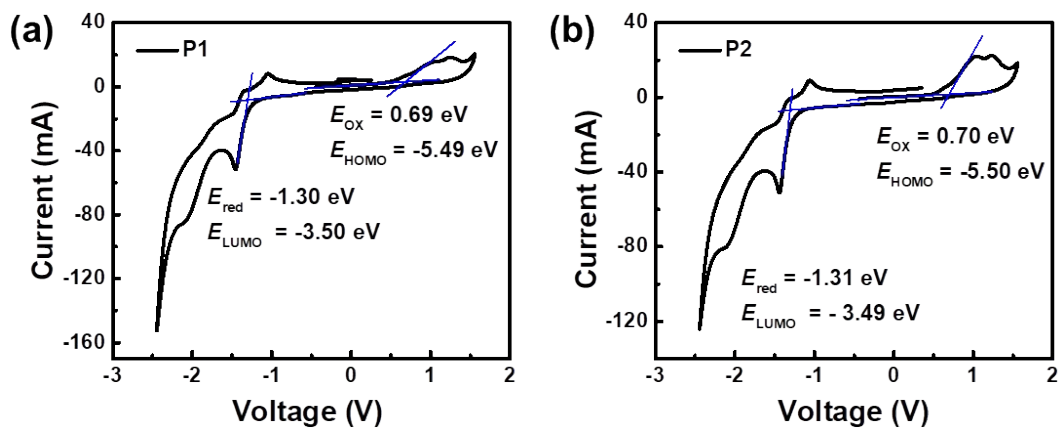


Figure S4. (a) Cyclic voltammogram of P1 thin film. (b) Cyclic voltammogram of P2 thin film. Potential vs. Fc/Fc^+ .

6. Solubility test

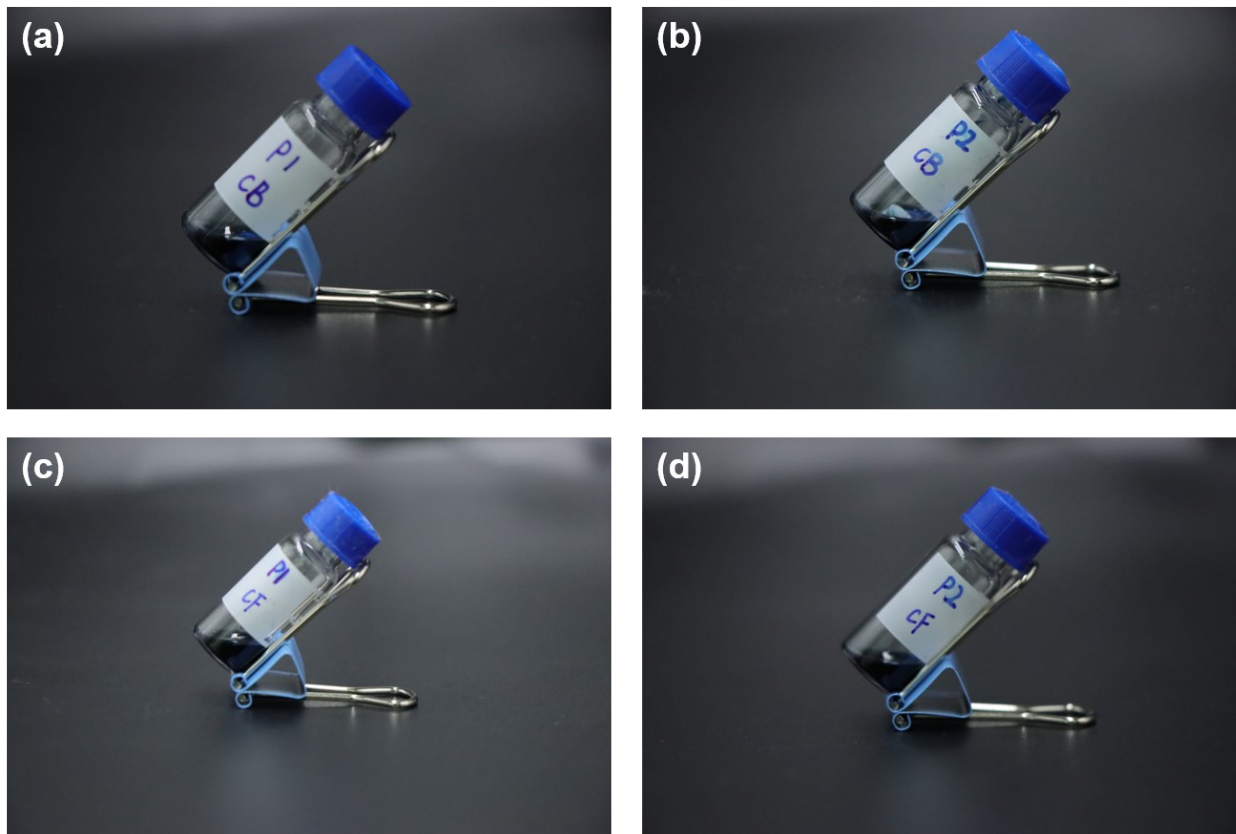


Figure S5. (a-d) The images of solutions based on P1 and P2. (a) P1 in CB with 10 mg/ml. (b) P2 in CB with 10 mg/ml. (c) P1 in CF with 8 mg/ml. (d) P2 in CF with 8 mg/ml.

7. Solar cells performance

Table S1. Characteristics of **P1** based solar cells spin coated from different thickness at the solution of CB and 150 °C annealing (10 min).

Thickness [nm]	J _{SC} [mA cm ⁻²]	V _{OC} [V]	FF	PCE [%]
30	4.67	0.81	0.36	1.37
40	5.00	0.80	0.35	1.39
50	4.26	0.79	0.34	1.13

Table S2. Characteristics of **P1** based solar cells spin coated from different annealing temperature at the solution of CB and the same thickness (40 nm).

Temperature [°C]	J _{SC} [mA cm ⁻²]	V _{OC} [V]	FF	PCE [%]
25	3.23	0.76	0.31	0.76
100	3.57	0.74	0.32	0.90
150	5.00	0.80	0.35	1.39
200	4.25	0.76	0.33	1.06

Table S3. Characteristics of **P1** based solar cells spin coated from different solution at the same thickness (40 nm) and 150 °C annealing (10 min).

Solvent	J_{SC} [mA cm ⁻²]	V_{OC} [V]	FF	PCE [%]
CB	5.00	0.80	0.35	1.39
CB/DIO (2%)	3.24	0.72	0.28	0.67
CB/DCB (3%)	3.24	0.74	0.34	1.24
CF	4.16	0.75	0.34	1.05

Table S4. Characteristics of **P2** based solar cells spin coated from different thickness at the solution of CB and 150 °C annealing (10 min).

Thickness [nm]	J_{SC} [mA cm ⁻²]	V_{OC} [V]	FF	PCE [%]
40	6.16	0.79	0.39	1.88
50	6.04	0.81	0.42	2.03
60	5.81	0.79	0.40	1.81

Table S5. Characteristics of **P2** based solar cells spin coated from different annealing temperature at the solution of CB and the same thickness (50 nm).

Temperature [°C]	J _{sc} [mA cm ⁻²]	V _{oc} [V]	FF	PCE [%]
25	3.83	0.80	0.37	1.12
100	4.69	0.82	0.40	1.55
150	6.04	0.81	0.42	2.03
200	6.07	0.76	0.41	1.89

Table S6. Characteristics of **P2** based solar cells spin coated from different solution at the same thickness (50 nm) and 150 °C annealing (10 min).

Solvent	J _{sc} [mA cm ⁻²]	V _{oc} [V]	FF	PCE [%]
CB	6.04	0.81	0.42	2.03
CB/DIO (2%)	5.96	0.79	0.38	1.77
CB/DCB (3%)	6.30	0.78	0.39	1.87
CF	3.72	0.74	0.37	1.02

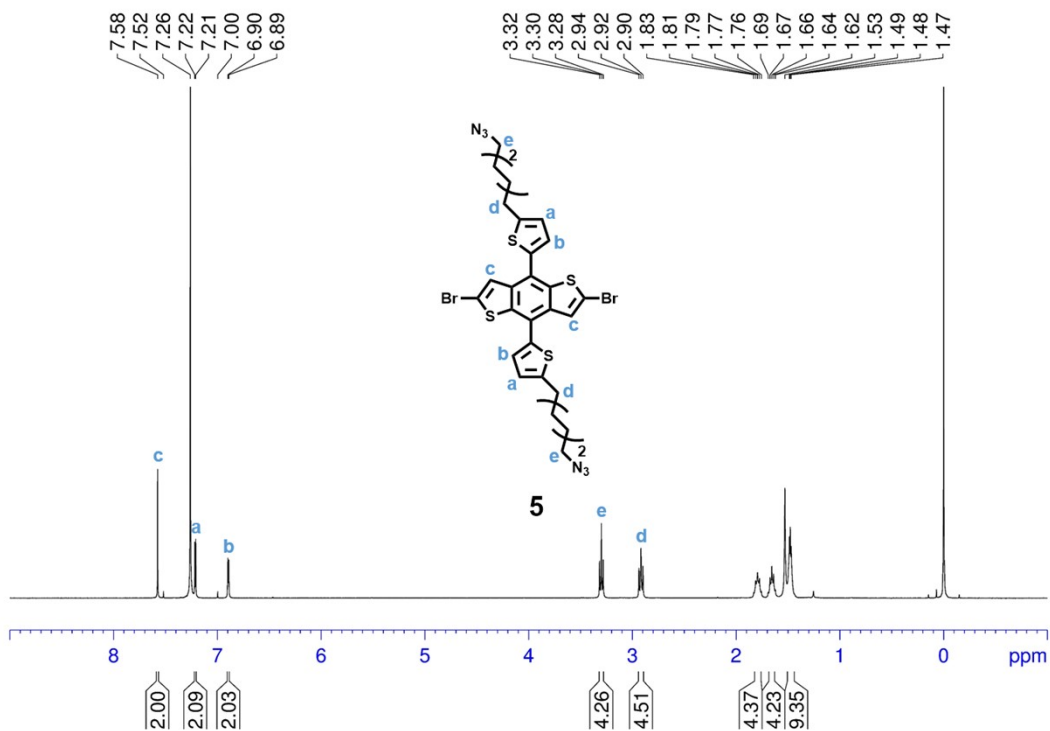
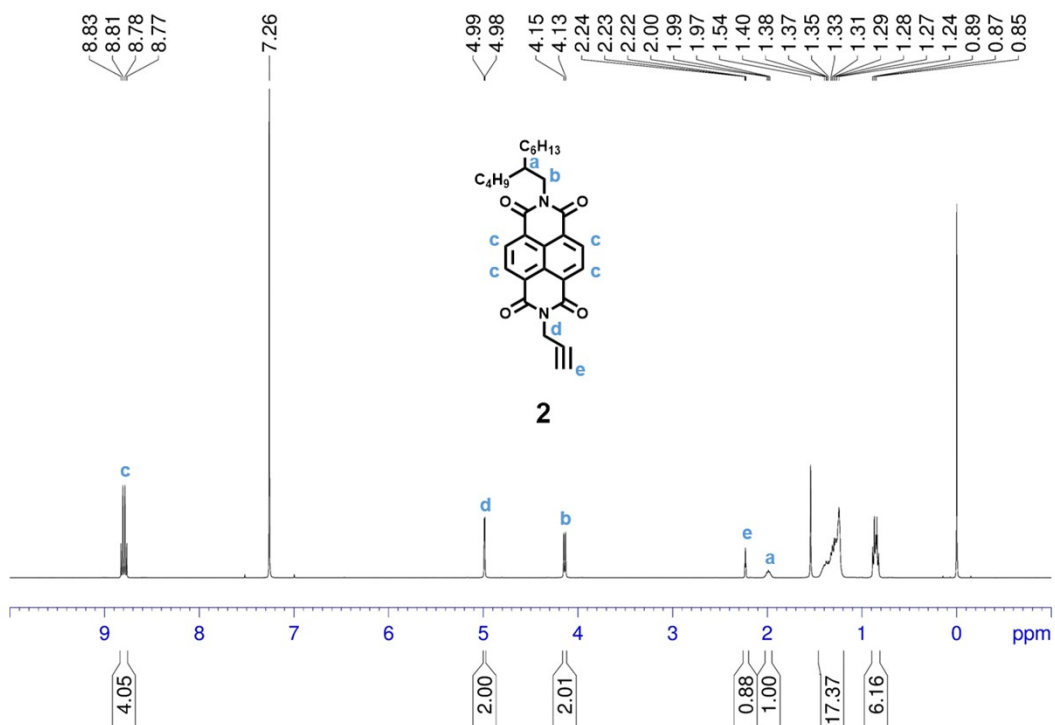
Table S7. Photovoltaic performances of 6 devices based on **P1** fabricated from CB annealed at 150 °C for 10 min.

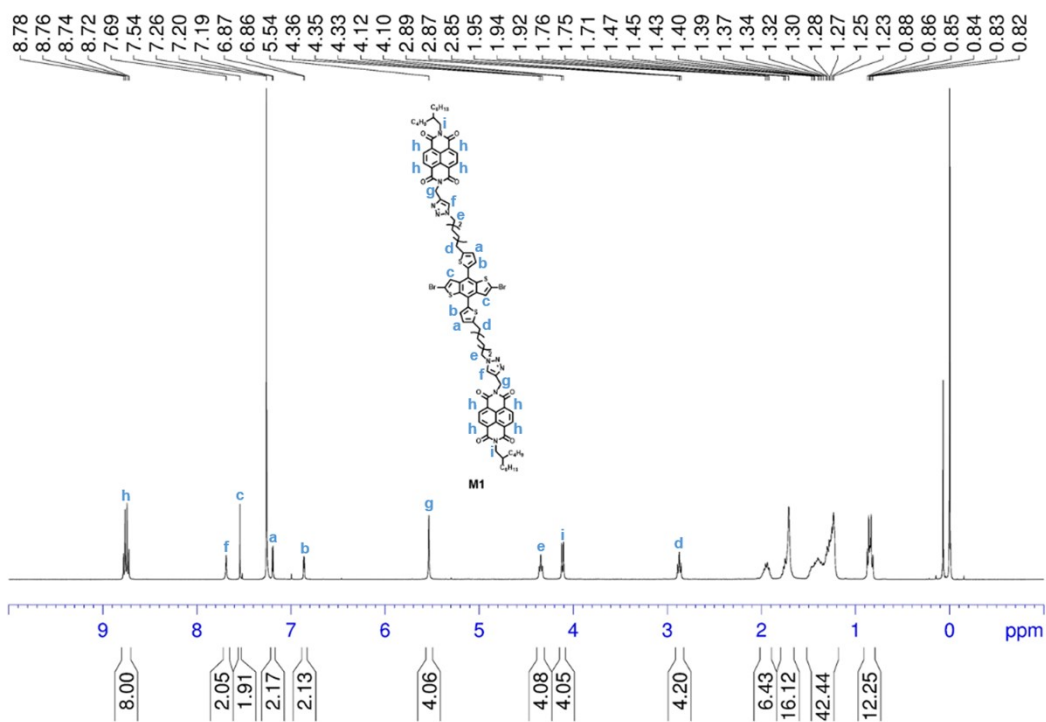
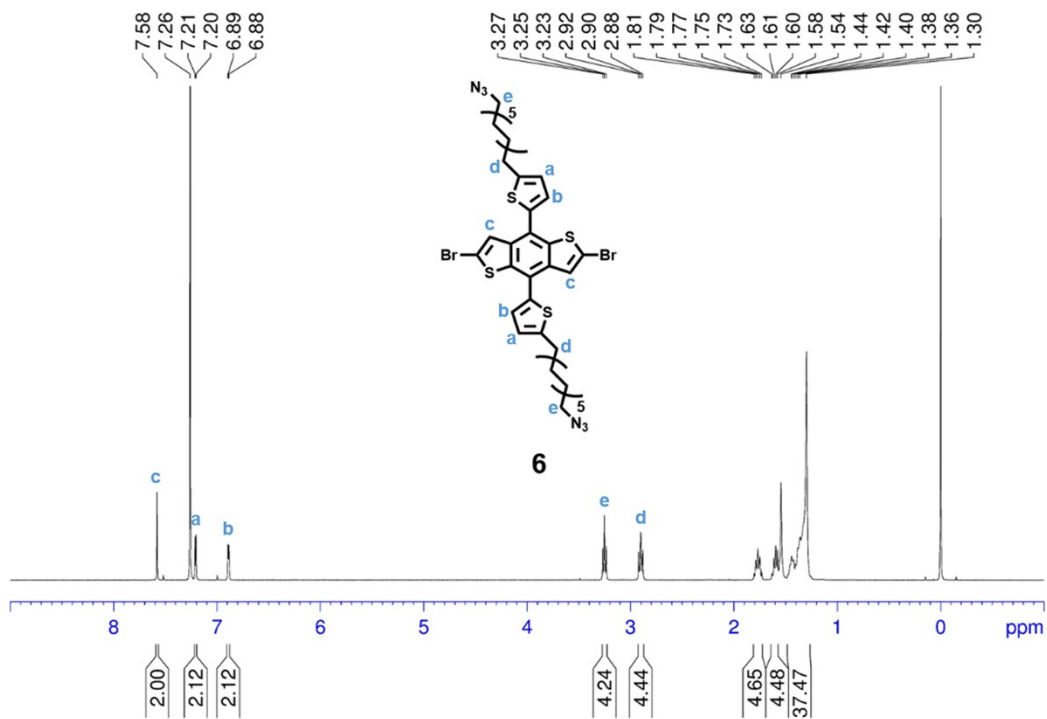
NO.	J _{SC} [mA cm ⁻²]	V _{OC} [V]	FF	PCE [%]
1	5.00	0.80	0.35	1.39
2	4.93	0.79	0.34	1.32
3	4.76	0.78	0.34	1.28
4	4.43	0.77	0.34	1.17
5	4.51	0.78	0.36	1.25
6	4.32	0.76	0.36	1.17
average	4.66±0.28	0.78±0.01	0.35±0.007	1.26±0.09

Table S8. Photovoltaic performances of 6 devices based on **P2** fabricated from CB annealed at 150 °C for 10 min.

NO.	J _{SC} [mA cm ⁻²]	V _{OC} [V]	FF	PCE [%]
1	6.05	0.81	0.42	2.03
2	6.04	0.80	0.42	2.00
3	6.31	0.80	0.41	2.08
4	6.26	0.79	0.40	2.00
5	6.34	0.80	0.41	2.08
6	6.24	0.80	0.40	1.97
average	6.21±0.13	0.80±0.01	0.41±0.007	2.03±0.05

8. NMR and MS of the compounds





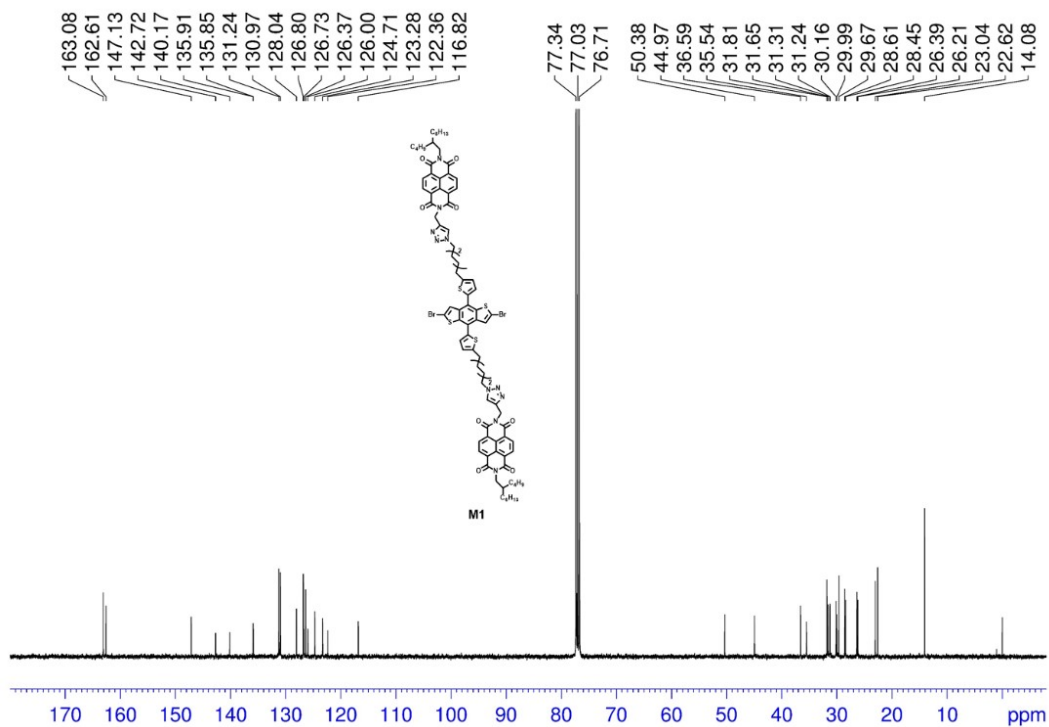


Figure S10. $^{13}\text{C-NMR}$ of the monomer **M1** recorded in CDCl_3 .

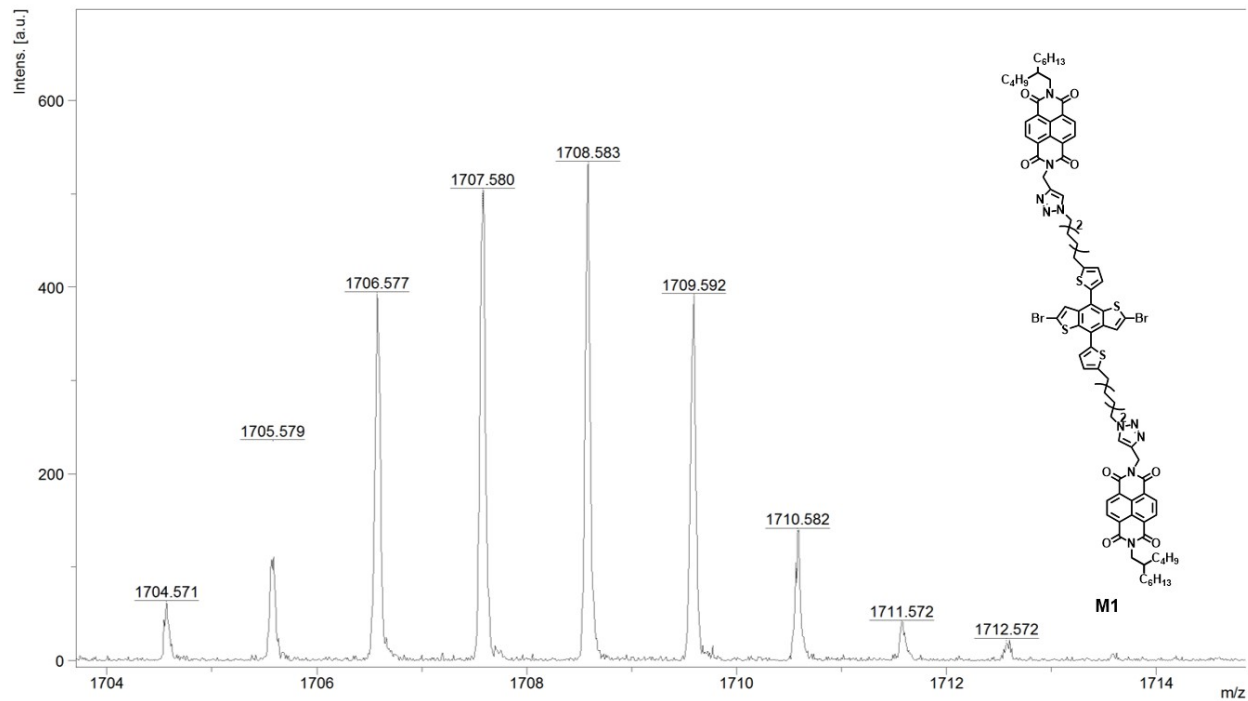


Figure S11. HRMS of the monomer **M1** recorded in CDCl_3 .

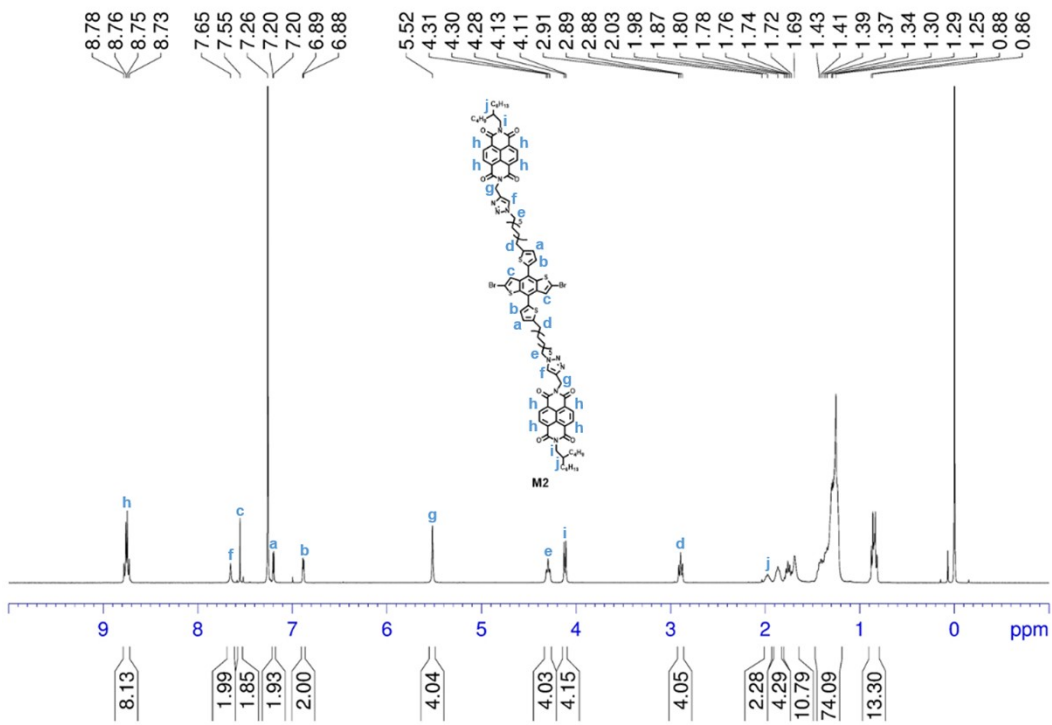


Figure S12. $^1\text{H-NMR}$ of the monomer **M2** recorded in CDCl_3 .

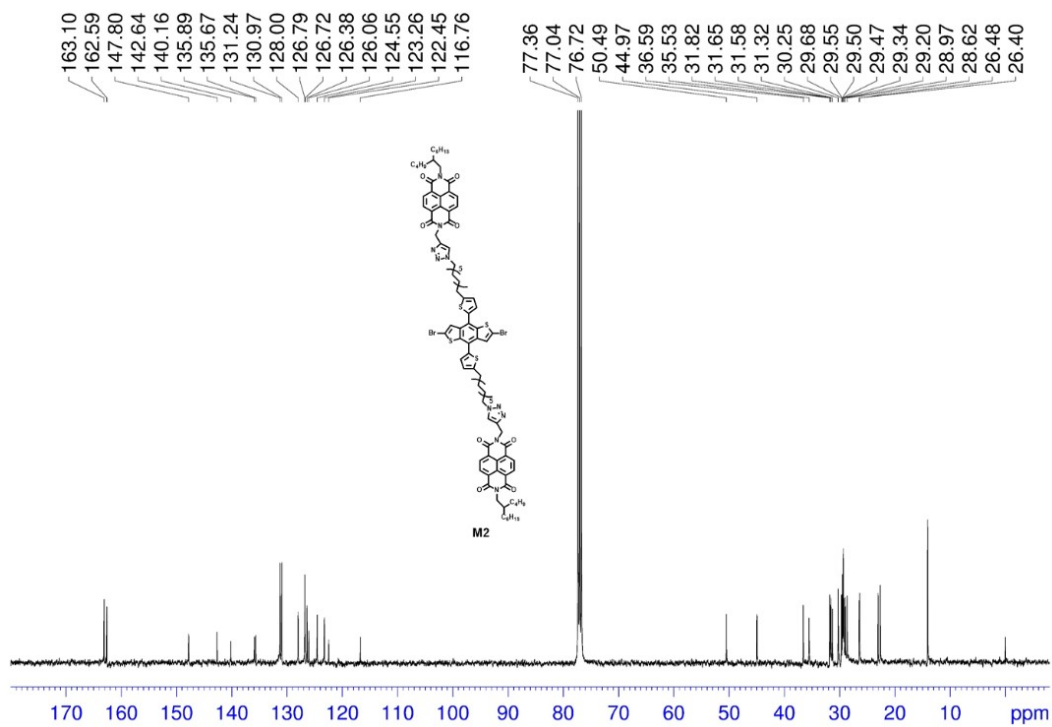


Figure S13. $^{13}\text{C-NMR}$ of the monomer **M2** recorded in CDCl_3 .

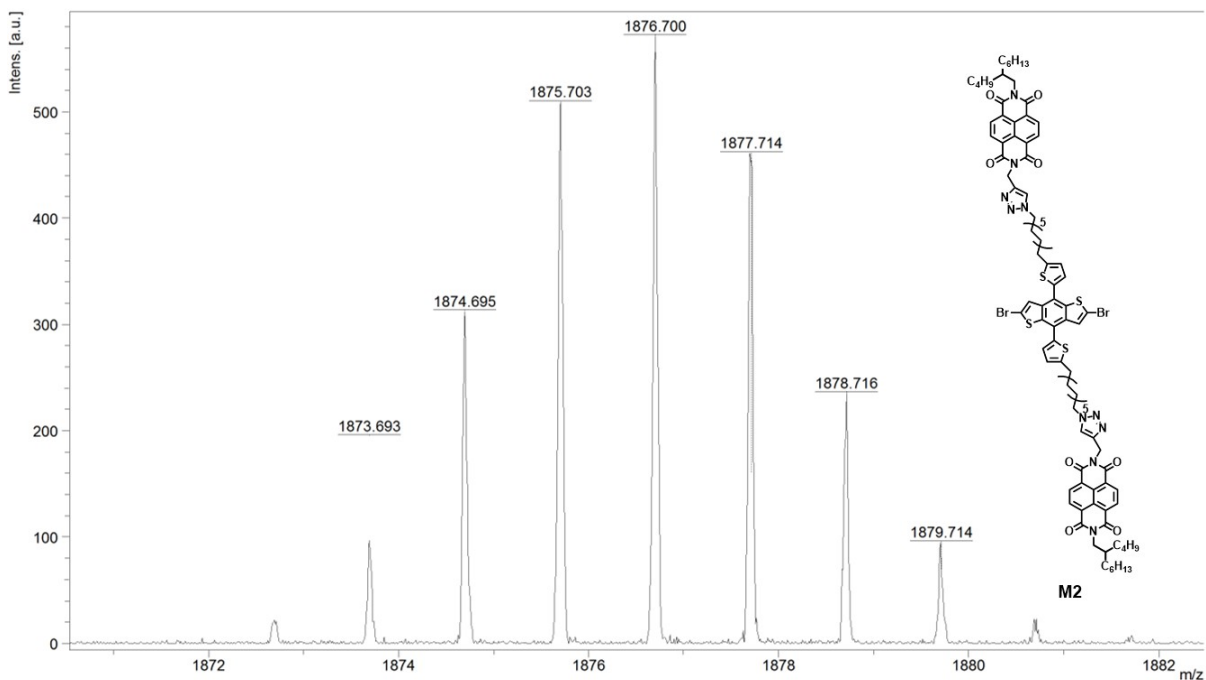


Figure S14. HRMS of the monomer **M2** recorded in CDCl_3 .

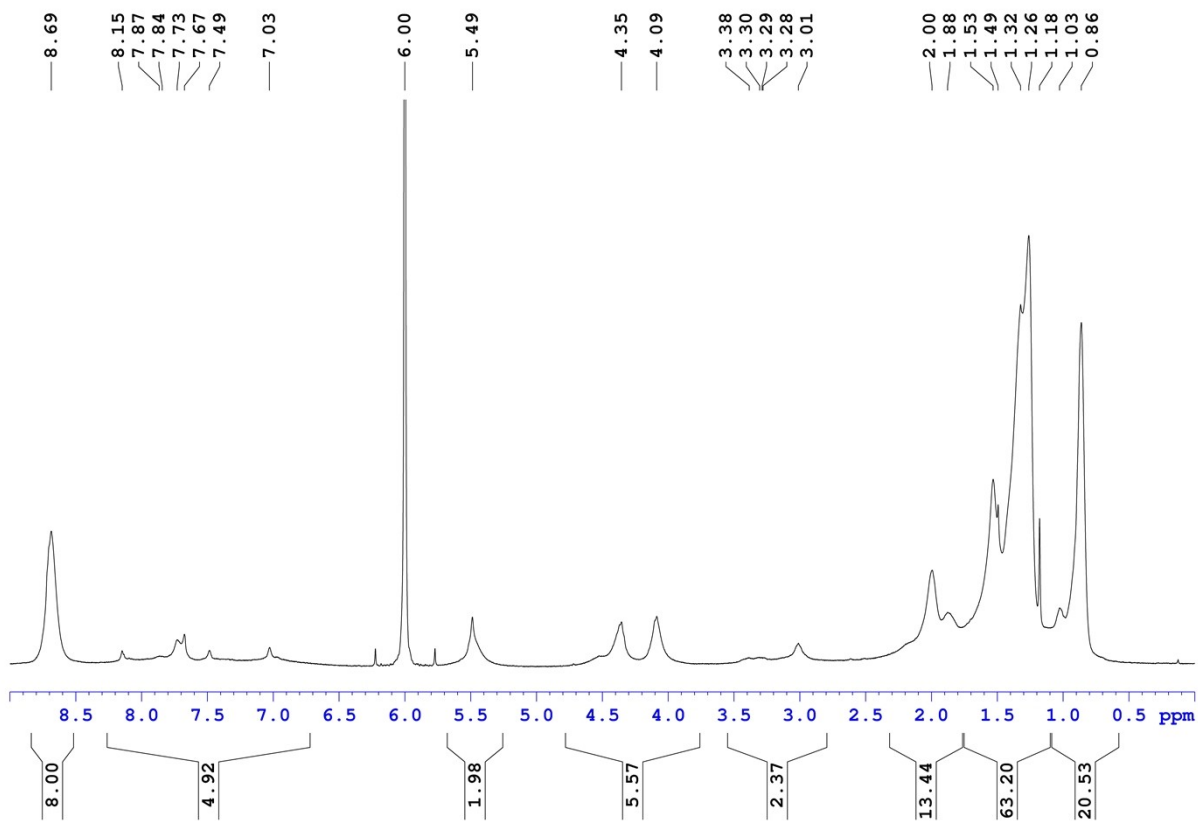


Figure S15. ^1H -NMR of the polymer **P1** recorded at $80\text{ }^\circ\text{C}$ with 1,1,2,2-tetrachloroethane- d_2 as the solvent.

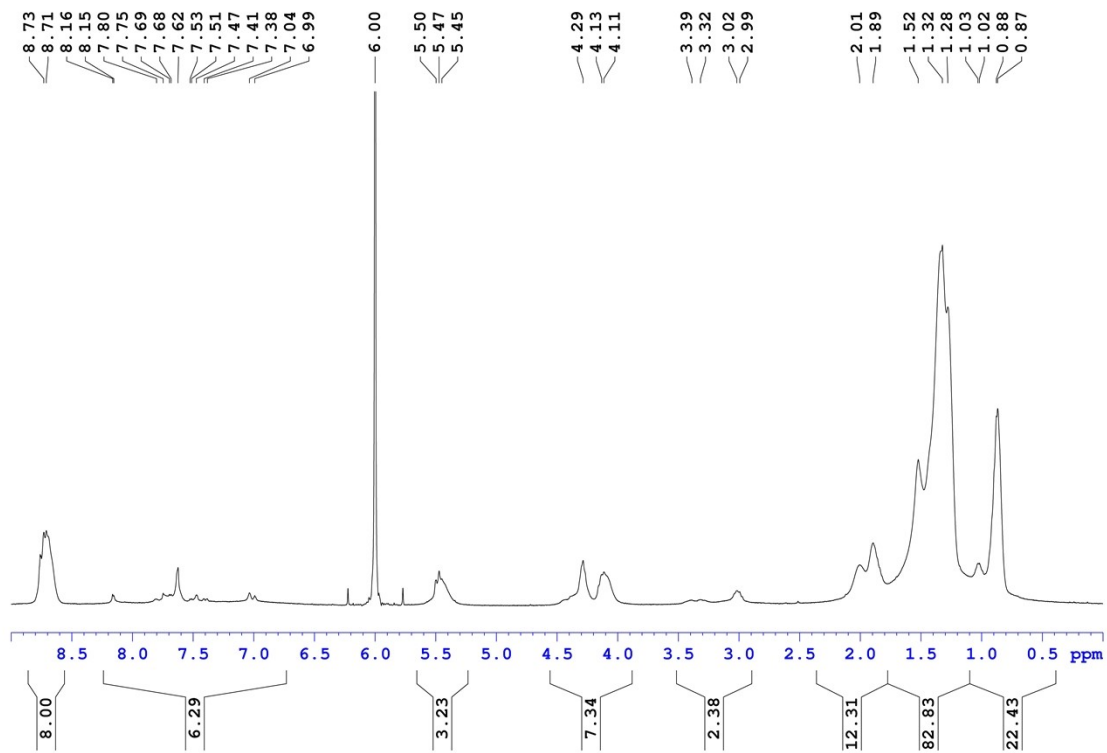


Figure S16. $^1\text{H-NMR}$ of the polymer **P2** recorded at $80\text{ }^\circ\text{C}$ with 1,1,2,2-tetrachloroethane- d_2 as the solvent.